Optimal Pattern Generator for Dynamic Walking in humanoid Robotics

David Galdeano, Ahmed Chemori, Sébastien Krut, Philippe Fraisse

D. Galdeano, A. Chemori, S. Krut and P. Fraisse

Optimal Pattern Generator for Dynamic Walking in humanoid Robotics

Abstract: This paper deals with an optimal Zero Moment Point (ZMP) based pattern generator for stable dynamic walking in humanoid robotics. The proposed method is based on a Three-Mass Linear Inverted Pendulum Model (3MLIPM), used as a simplified model of the biped robot. The 3MLIPM considers the biped robot as a three point masses and two-link system. A ZMP based performance index is then used in an optimization problem whose solution gives the best values of the model's parameters w.r.t. dynamic walking stability. Numerical simulations are presented to show the effectiveness of the proposed optimal pattern generator for the case of the biped walking robot SHERPA.

Keywords: Biped walking robot, Pattern generation, Three-mass linear inverted pendulum model, Optimization.

1 Introduction

A humanoid robot is a robot with an appearance based on that of the human body. Humanoids walking is a very challenging field of research due to the complexity of synthesizing stable gaits for these systems. Indeed, within this field, humanoid robot control needs sophisticated control schemes to deal with their complexity including:

- the high-order nonlinear dynamics,
- the variable structure model according to the different phases of the walking cycle,
- the contact constraints with the ground that should be managed,
- the hybrid character of the dynamics due to rigid impacts between the robot's foot and the ground,
- the stability during walking that should be ensured.

Most of the proposed control schemes in the literature are based on the use of some reference trajectories that should be tracked in real-time. This fact shows the importance of a pattern generator in humanoid walking control. Several types of pattern generators have then been proposed in the literature. However, those who

D. Galdeano, A. Chemori, S. Krut and P. Fraisse: LIRMM, Université Montpellier 2, LIRMM, Montpellier, France, emails: galdeano@lirmm.fr, chemori@lirmm.fr, krut@lirmm.fr, fraisse@lirmm.fr.

De Gruyter Oldenbourg, ASSD – Advances in Systems, Signals and Devices, Volume 1, 2016, pp. 115–139.
DOI: 10.1515/9783110448375-008

guarantee an *a-priori* walking stability are often based on one of the following stabilization criteria:

- The Center Of Mass (COM)
- The Zero Moment Point (ZMP)
- The Foot Rotation Indicator (FRI)

The COM [1] is the mean location of all masses of the robot links. It is usually used as a static stability criterion. The ZMP [2, 3] is the point of junction between the center of the vertical reaction forces and the ground. It is the most used dynamic stability criterion. The FRI [4] is a point on the foot/ground-contact surface where the net ground-reaction force would have to act to keep the foot stationary. It is an indication of postural stability and, in case of instability, indicates how the robot will fall. It is used as a dynamic stability criterion.

2 Related works

In the literature several methods have been proposed for generating walking trajectories in humanoid robotics.

A method based on a motion capture of human walking has been proposed in [5]. This method can gives human-like motions, however its main drawback lies in the captured data that can be hard to adapt to the humanoid robot.

Another method of trajectory generation for stable dynamic walking is proposed in [6]. It consists in using a 3^{rd} order spline function to generate feet and hip trajectories. The foot trajectories can be adapted to the ground variations to generate a stable dynamic walking on a rough terrain.

In [7] another pattern generation method has been proposed. It consists in using Fourier series to generate stable walking, with an iterative procedure to guarantee the stability. The main drawback of such a method lies in the computation time that does not enable a real-time implementation.

Another interesting method is the so called Inverted Pendulum Model (IPM) [8, 9] that considers the robot as a single point mass and massless legs. This method simplifies the dynamics of the robot to an inverted pendulum with a point mass linked by a telescopic leg to a spherical ground/leg joint.

The Linear Inverted Pendulum Model (LIPM) [10, 11] is an extension of the IPM where the height of the torso is considered to be constant leading to a more natural movement.

The IPM ignores the dynamics of the legs since it considers the stance leg as an inverted pendulum with a point mass. This fact can involve a loss of walking stability since the considered model is considerably simplified and consequently not sufficiently accurate. For instance, this is the case when the robot has heavy legs or

has no torso (case of our robot SHERPA). In order to approximate the robot with a more accurate model, it would be necessary to consider the whole-body dynamics by using a preview control to correct the error between the IPM and the real robot as in [12] or to use a multiple point mass model instead of considering a one point mass model.

For instance, a Two-Mass Inverted Pendulum Model (TMIPM) and Multiple Mass Inverted Pendulum Model (MMIPM) extending the IPM were proposed in [13]. In the MMIPM, the considered model is composed by more than one mass. These masses are located at the hip and along the swinging leg in the case of a two-mass model.

The Gravity-Compensated Inverted Pendulum Model (GCIPM) [14] uses also one mass to represent the body of the robot and an additional mass to represent the swing leg.

A three-mass model using the concept of ZMP has been studied in [15]; however, it doesn't use any LIPM to generate trajectories and the torso of the biped robot moves up and down.

A generation of walking trajectories using a three point mass model to calculates center of mass trajectories from footstep locations has been proposed in [16]. This approach use offline optimization of some free geometrical parameters like the trunk angular motion w.r.t. the speed of the robot. These parameters are then used in a real-time fast planning to compute the reference torque patterns to apply on the robot.

Another three-mass model using the inverted pendulum concept is proposed in [17]. However, it has one important drawback related to the geometrical parameters, such as the position and the location of masses, which have been chosen arbitrarily. One good idea would then be to tune these parameters at their best values in order to enhance the walking stability of the robot, and this is the scope of the present paper.

The proposed solution is an extension of the method proposed in [17] to deal with dynamic stability of walking in the generated trajectories, as well as changes in direction during walking. As in [17], the robot's dynamics will be approximated by a Three-Mass Linear Inverted Pendulum. The hip and feet trajectories are generated by the movement of masses. The walking movement of the robot is generated in the sagittal and frontal planes separately. The joint trajectories are computed using inverse kinematics of the biped robot. In order to ensure a stable dynamic walking, the parameters of the model must be well tuned. The best way to perform such a tuning is through an optimization of the generated joints' trajectories to minimize the ZMP excursion within the footprint which will increase the stability margins. The second contribution of this work is to propose online change of walking direction, where new optimal trajectories are generated to ensure *a-priori* stability during walking while turning.

This paper is organized as follows: in the next section, the prototype of our demonstrator SHERPA is introduced. Section 4 introduces the simplified model that will be used in the generation of the reference trajectories and how it was used in the pattern generator proposed in [17]. In section 5, the proposed extension of this

method is presented, where our contributions are highlighted. Numerical simulations are presented and discussed in section 6, where the effectiveness of the proposed method is shown and compared with the original one for the case of SHERPA robot. The paper ends with some concluding remarks.

3 Description of SHERPA prototype

The SHERPA walking robot (cf. Fig. 3) is a French biped robot developed at the LIRMM laboratory [18] within the framework of the national project ANR-06-BLAN-0244 SHERPA. The name of this robot comes from the so-called Sherpa, who are members of a people of Tibetan stock living in the Nepalese Himalayas, and who often serve as porters on mountain-climbing expeditions. Indeed, this robot is built to carry loads while walking in a human environment [19].

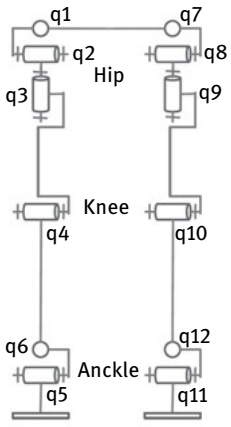

Fig. 1. SHERPA kinematics model.

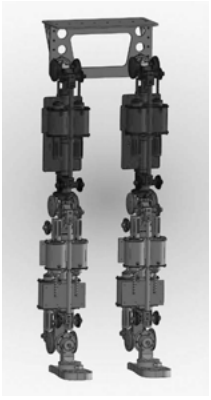

Fig. 2. CAD model of SHERPA.

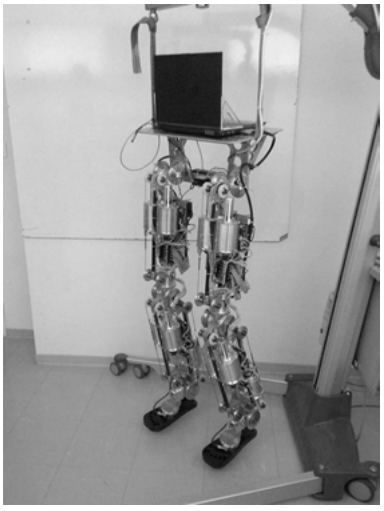

Fig. 3. The SHERPA robot.

SHERPA is composed of a hip linking two legs together. Each leg has six degrees of freedom (dof), and the robot is equiped with 12 actuators, which is enough to reproduce a human gait.

These dofs are distributed on the different articulations of the robot as follows: three dofs at the hip, one dof at the knee and two dofs at the ankle as it is illustrated on Fig. 1. The geometric parameters of the robot are summarized in Tab. 1.

Tab. 1. Geometric parameters of SHERPA biped robot.

Description	Parameter	Value
Length of thigh	L_{thigh}	0.5033 m
Width of the hip	L_s	0.31 m
Total weight of the robot	*mass*	47.1 kg

This robot differs basically from the other walking robots by its actuation system, which is transparent (backdrivable, with low inertia), and organized in modules (as illustrated in Figs. 4–5).

Each actuation module includes two actuators acting in parallel on two dofs simultaneously. The mechanical transmission of these modules is such that when the two actuators work together on the joint, they cause the movement of the first dof; and when they act in opposite directions they cause the movement of the second dof. These modules are equipped with custom-made electric motors.

The transmission of movement is based on the use of a ball screw transforming the rotation of the hollow shaft electrical actuator in a translational movement. This last one is then transmitted to pulleys using cables to produce the desired rotational movement. This basic principle of motion transmission is illustrated in Fig. 6.

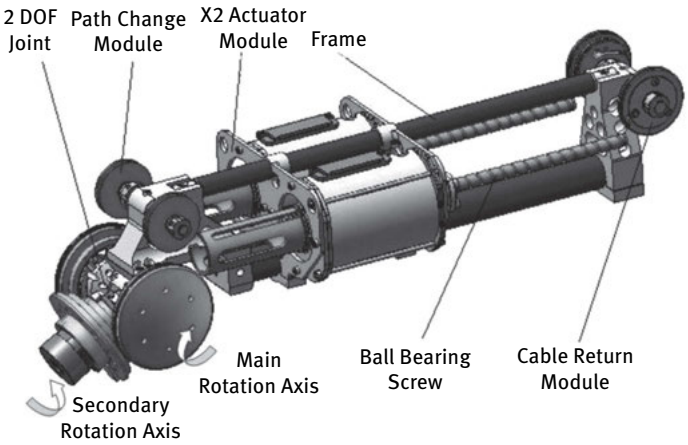

Fig. 4. CAD view of an actuator module.

This technology gives the robot's actuators remarkable characteristics such as no backlash, low friction, reversibility of the chain of transmission and low inertia.

The kinematic model of SHERPA robot is created through the link representation proposed in [20]. This model uses the twelve joints' values as well as the position and

orientation of the hip to generate the Cartesian position of each articulation in the operational space.

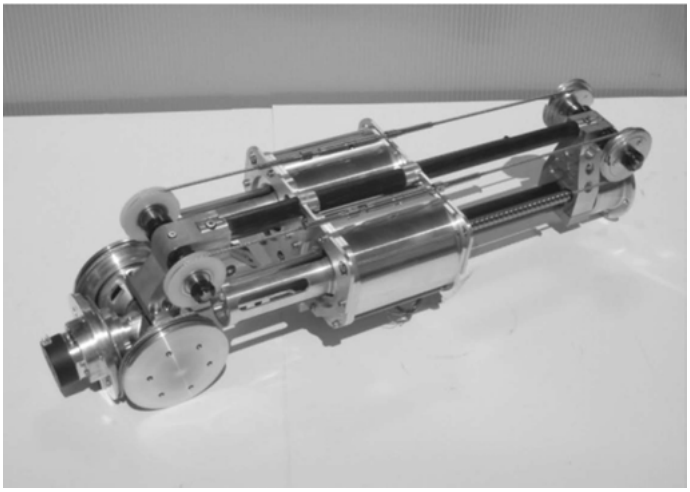

Fig. 5. View of a real manufactured module.

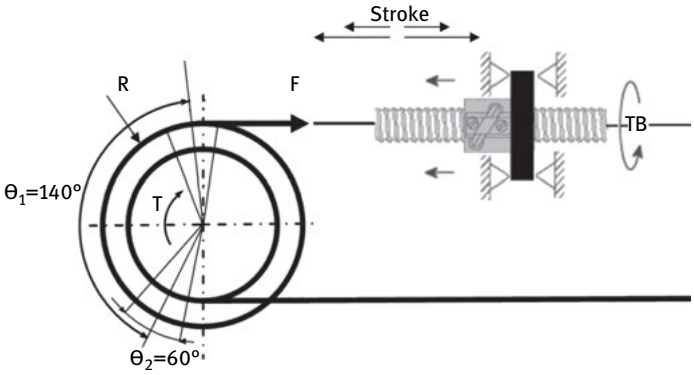

Fig. 6. Cable/Pulley transmission system used in actuation module of SHERPA.

The forward kinematics model writes:

$$X = f(q) \tag{1}$$

where $X \in \mathbb{R}^{39\times1}$ includes Cartesian positions of articulations and the hip's center position, $q \in \mathbb{R}^{18\times1}$ includes a 12×1 vector of joints positions, and a 6×1 vector of the position and orientation of the hip.

The inverse kinematic model is obtained by solving an analytical equation to find the articular positions expressed in terms of operational space positions of the hip and feet. The inverse kinematic model can then be written as:

$$q = g(X_r) \tag{2}$$

where $X_r \in \mathbb{R}^{9\times1}$ represents the operational space position of the hip (3×1) and the feet (6×1). The orientation of the hip and the feet are kept constant and equal to zero.

The computation of the ZMP and CoM of the robot is based on the formalism presented in [20], in which the ZMP evaluation uses the angular momentum with the overall dynamic model of the robot.

4 Three-mass linear inverted pendulum model

The three-mass Linear Inverted Pendulum Model (3MLIPM) as introduced in [17] simplifies the biped robot to a three-link system (as shown in Fig. 7) with a point mass on each link. The three masses represent the torso and the two legs, unlike the single mass model (as in IPM or LIPM) where a unique mass is located at the hip of the robot. The three links are connected together at the hip.

This model is more accurate than the single mass model, especially for biped robots without torso, where the position of the CoM can be very different from the hip position.

From Fig. 7, the equations of moment applied on the supporting ankle can be formulated as follows:

$$\tau_x = \sum_{i=1}^{3} m_i(g + \ddot{z}_i)y_i - \sum_{i=1}^{3} m_i\ddot{y}_i z_i \tag{3}$$

$$\tau_y = \sum_{i=1}^{3} m_i\ddot{x}_i z_i - \sum_{i=1}^{3} m_i(g + \ddot{z}_i)x_i \tag{4}$$

where τ_x and τ_y are the torques applied on the ankle, m_i represents the value of the i^{th} point mass, (x_i, y_i, z_i) are the Cartesian positions of the i^{th} point mass ($i = 1, 2$ or 3 represent respectively the stance leg, the torso and the swing leg), $(\ddot{x}_i, \ddot{y}_i, \ddot{z}_i)$ are their corresponding accelerations.

For simplification, the height of the masses is assumed to be constant and the torque applied on the supporting ankle is assumed to be zero [17]. With these

assumptions, (3) and (4) can be simplified into:

$$\sum_{i=1}^{3} m_i \ddot{y}_i z_i = \sum_{i=1}^{3} m_i g y_i \text{ and } \sum_{i=1}^{3} m_i \ddot{x}_i z_i = \sum_{i=1}^{3} m_i g x_i \tag{5}$$

These equations are decoupled, so the movement can be generated in sagittal and lateral planes separately.

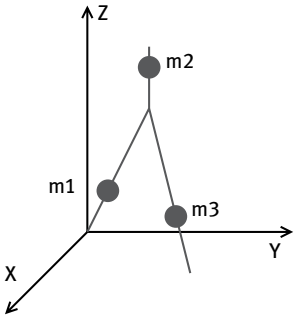

Fig. 7. Graphical representation of the Three-Mass Linear Inverted Pendulum Model.

4.1 Assumptions and notations

The following assumptions are considered to simplify the calculations [17]:
- The ground is flat and horizontal.
- The height variation of each mass can be neglected.
- The double support phase is considered instantaneous.
- There is no energy loss during impact.
- The standing foot has no overturn when touching and leaving the ground.
- The swing foot is parallel to the ground.
- The torso is upright.

Besides, the following notations are used:
- $2T$: The whole stepping cycle.
- $2D_s$: The steeping length.
- L_s: The width of a step.

4.2 Motion study in the sagittal plane

The movement in the sagittal plane and the associated notations are illustrated in Fig. 8.

With the above assumptions, heights and masses can be normalized as follows:

$$z_2 = \gamma z_1 \ , \ z_3 = z_1 \ , \ x_2 = \lambda x_1 \ , \ m_2 = k m_1 \ , \ m_3 = m_1 \tag{6}$$

where γ, λ and k are the parameters extracted from the robot's model. Considering (6), equation (5) can be simplified into:

$$b\ddot{x}_1 + d\ddot{x}_3 = a x_1 + x_3 \tag{7}$$

$$a = k\lambda + 1, \quad b = \frac{z_1}{g}(1 + k\gamma\lambda), \quad d = \frac{z_1}{g} \tag{8}$$

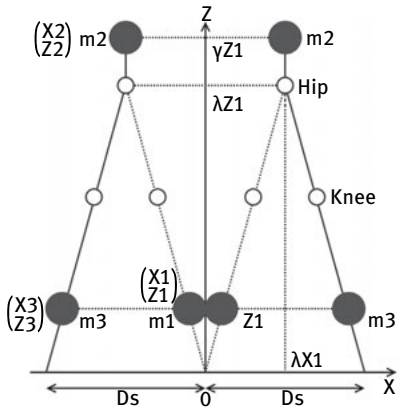

Fig. 8. Illustration of movement in the sagittal plane.

In order to generate walking gaits, a trajectory for the swing foot (mass m_3) is necessary. If the trajectory of this last one is known, then those of the two other masses can be computed. According to [17], a sinusoidal function is chosen to represent the trajectory of the mass m_3, as follows:

$$x_3 = A\cos(\omega t + \phi) \tag{9}$$

where parameters ϕ and A are given in the sequel by equation (13). Here, ω is not the step frequency, it is a parameter that must be chosen to keep the foot position and velocity positive in order to ensure a forward movement of the foot during the step.

Using (7) and (9), x_1 can be expressed by:

$$x_1 = C_1 \cos(\omega t + \phi) + C_2 e^{\sqrt{\frac{a}{b}}\, t} + C_3 e^{-\sqrt{\frac{a}{b}}\, t} \tag{10}$$

With the above assumptions given in section 4.1, initial conditions can be fixed as:

$$x_1(0) = -\frac{D_s}{2\lambda}, \quad x_3(0) = -\frac{D_s}{2\lambda}(2\lambda - 1) \tag{11}$$

$$x_1\left(\frac{T}{2}\right) = 0, \quad x_3\left(\frac{T}{2}\right) = 0 \tag{12}$$

The equations' coefficients can then be identified using initial conditions:

$$\phi = -\frac{\pi}{2} - \frac{T}{2}\omega, \quad A = -\frac{D_s(2\lambda - 1)}{2\lambda \cos\phi} \tag{13}$$

$$C_1 = -\frac{A(1 + d\omega^2)}{a + b\omega^2} \qquad C_3 = -e^{\sqrt{\frac{a}{b}}\, t} C_2 \tag{14}$$

$$C_2 = \frac{1}{1 - e^{\sqrt{\frac{a}{b}}\, t}} \left(-\frac{D_s}{2\lambda} - C_1 \cos\phi\right) \tag{15}$$

With all trajectories of point masses computed, the trajectories of the hip and ankles can then be determined using geometrical constraints from Fig. 8.

$$\begin{aligned} &x_{st}(t) = 0 \ \text{ for } \ 0 \le t \le T, \ x_h(t) = \lambda x_1(t) \ \text{ for } \ 0 \le t \le T \\ &z_{st}(t) = 0 \ \text{ for } \ 0 \le t \le T, \ z_h(t) = \lambda z_1 \quad \text{ for } \ 0 \le t \le T \end{aligned} \tag{16}$$

where x_{st}, z_{st} represent Cartesian positions of the stance foot along x and z axis respectively. x_h, z_h are the Cartesian positions of the hip along x and z axis respectively.

During the step, the vertical position of the swing foot needs to be higher than the floor. A sinusoidal shape can then be an appropriate function for the swing foot trajectory along the z axis. However, due to the previous assumptions, the influence of this change of height is neglected in computations.

$$\begin{aligned} x_{sw}(t) &= \frac{\lambda x_3(t) - \lambda x_h(t)}{\lambda - 1} \qquad \text{for } \ 0 \le t \le T \\ z_{sw}(t) &= \frac{\sqrt{2} H_s}{2} \sqrt{1 + \sin\left(\frac{2\pi}{T} t - \frac{\pi}{2}\right)} \ \text{ for } \ 0 \le t \le T \end{aligned} \tag{17}$$

where x_{sw}, z_{sw} are the positions of the swing foot along the x and z axis respectively, and H_s is the maximal height of the swing foot during walking.

4.3 Motion study in frontal plane

The movement in the frontal plane and the associated notations are illustrated in Fig. 9.

The 3MLIPM equations are now derived in the frontal plane.

$$u\ddot{y}_1 - vy_1 = w \tag{18}$$

Where the coefficients u, v and w are given by:

$$u = (2 + k\lambda\gamma)\frac{z_1}{g},\ v = (2 + k\lambda),\ w = \left(L_s + k\frac{L_s}{2}\right) \tag{19}$$

These equations are solved considering the following initial conditions:

$$y_1(0) = 0, \quad \dot{y}_1\left(\frac{T}{2}\right) = 0, \quad y_1(T) = 0 \tag{20}$$

The trajectory of the mass m_1 along the y axis is then computed and expressed by:

$$y_1(t) = C_1 e^{\sqrt{\frac{v}{u}}t} + C_2 e^{-\sqrt{\frac{v}{u}}t} - \frac{w}{v} \tag{21}$$

where:

$$C_1 = \frac{w}{v}\frac{1 - e^{\sqrt{\frac{v}{u}}T}}{1 - e^{2\sqrt{\frac{v}{u}}T}},\ C_2 = e^{\sqrt{\frac{v}{u}}t}C_1 \tag{22}$$

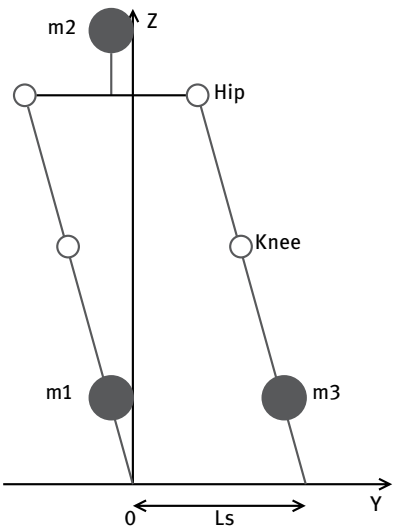

Fig. 9. Illustration of movement in the frontal plane.

Once the trajectory of the mass m_1 is computed, those of m_2 and m_3 can be easily determined using geometrical constraints illustrated on Fig. 9. From these trajectories and the inverse kinematics of the robot, the trajectories of all the joints of the robot can then be computed.

4.4 Adaptation of the general model for SHERPA robot

The SHERPA robot is a biped robot without a torso (cf. Fig. 3). In order to simplify the model, the torso point mass is set on the hip. This modification results in $\gamma = \lambda$.

It is worth to note that the basic principle of the proposed method in [17] and summarized above uses some geometrical parameters of the robot (such as m_1, m_2, m_3 and z_1, z_2, z_3) but doesn't give a method to calculate them. In order to take into account the dynamic stability of the resulting walking trajectories, we propose to tune these parameters using optimization to enhance the walking performance. The idea of such contribution is detailed in the following section.

5 Reference trajectories optimization

The proposed pattern generator in [17] computes joint reference trajectories using arbitrary defined parameters. This can be improved by choosing the best values of some of them (namely m_1 and z_1) to ensure walking stability. Since we are interested in dynamic walking, the position of the Zero Moment Point (ZMP) [2] is then used as an indicator of stability.

5.1 Dynamic stability margins

The stability margins are defined by the distance to the limit of stability (i.e. the boundary of the footprint), they are illustrated in Fig. 10.

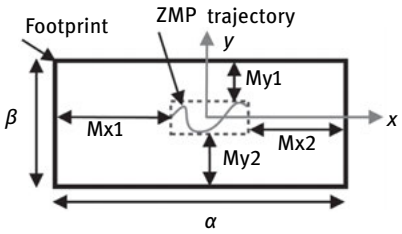

Fig. 10. ZMP displacement inside the footprint and stability margins.

The dashed interior rectangle explicits the boundaries of the ZMP displacements. Based on Fig. 10, the stability margins can be mathematically expressed as follows:

$$\begin{aligned} Mx_1 &= \frac{\alpha}{2} + \min(dZMP_x(t)),\ Mx_2 = \frac{\alpha}{2} - \max(dZMP_x(t)) \\ My_1 &= \frac{\beta}{2} + \min(dZMP_y(t)),\ My_2 = \frac{\beta}{2} - \max(dZMP_y(t)) \\ &\forall \quad t \in [ts_i\ ,\ ts_f] \\ Mx &= \min(Mx_1, Mx_2),\ My = \min(My_1, My_2) \end{aligned} \tag{23}$$

were $dZMP_x(t)$ and $dZMP_y(t)$ are the deviations of the ZMP trajectory with respect to the center of the stance foot along x axis and y axis respectively, ts_i and ts_f are the time instants of landing and lift-off of the stance foot respectively. The duration of the step is $T = ts_f - ts_i$.

5.2 Optimization w.r.t. dynamic walking stability

The first main contribution of this paper is to improve the pattern generator proposed in [17] by considering an optimization criterion in order to find the best values of z_1 and m_1 to enhance the dynamic walking stability.

In order to do that, the ZMP corresponding to the generated joint trajectories should be computed with the overall dynamics of the robot and compared with the desired ZMP, set to the center of the stance foot. This chosen ZMP desired position corresponds to a maximum stability margins.

The following objective function is then proposed to be optimized w.r.t. the parameters z_1 and m_1:

$$\begin{bmatrix} \hat{z}_1 \\ \hat{m}_1 \end{bmatrix} = \arg \min_{\begin{bmatrix} z_1 \\ m_1 \end{bmatrix}} \max \left(\sqrt{\frac{1}{\alpha}(x_{zmp} - x_{dzmp})^2 + \frac{1}{\beta}(y_{zmp} - y_{dzmp})^2} \right) \tag{24}$$

where x_{zmp} and y_{zmp} are the positions of the computed ZMP, x_{dzmp} and y_{dzmp} are those of the desired one. z_1 and m_1 are the optimization parameters, α and β are the length and the width of the foot (i.e. along x axis and y axis respectively, cf. Fig. 10).

By minimizing the maximum normalized deviation of the ZMP trajectory as cost function, the objective function computes the mass distribution to ensure the largest stability margins.

5.3 Change of direction and stability optimization

One key feature of a pattern generator is to allow the biped robot to change the walking direction using the kinematic model like in [21], or the dynamic model as in [22] with a two point mass system model.

As proposed in [17], the original 3MLIPM pattern generator is designed to make the robot walking only in a straight line. Our second contribution is then to modify it to allow a change of direction while walking. The change of direction is obtained through the application of a rotation at the hip of the stance leg, as follows:

$$\Omega = -\frac{R}{2}\cos\frac{\pi t}{T} \tag{25}$$

with Ω is the angle of rotation and R is its amplitude.

The change of direction alters the stability of the biped robot. Therefore, the proposed optimization criterion (24) is used again to improve dynamic walking stability. The solution of this optimization problem gives the best values for z_1 and m_1 which allow a better dynamic stability of the robot walking and turning.

6 Simulation results

A simulator for SHERPA biped robot was developed using the Graphical User Interface of Matlab™software. Its graphical interface is shown in Fig. 11.

This interface enables the tuning of some parameters of the robot as well as those of the optimization criterion. A graphical animation of the robot or the three mass model can also be displayed in the simulator to show the obtained movements.

The parameters z_1 and m_1 are computed by optimization, the other parameters are constant and summarized in Tab. 2.

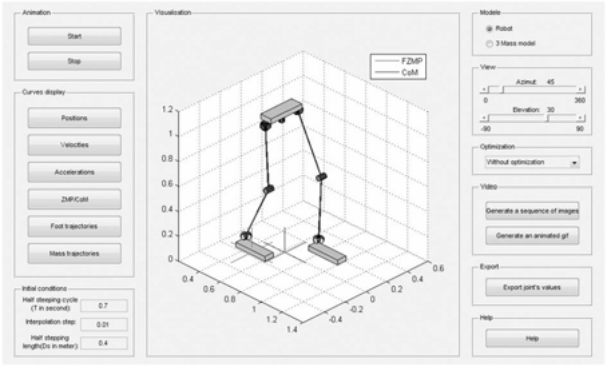

Fig. 11. View of the Graphical User Interface of SHERPA biped robot simulator.

Tab. 2. Parameters of the 3 MLIPM pattern generator.

Description	Parameter	Value
Weight of one leg	m_1	Optimized
Weight of the torso	m_2	$mass - 2m_1$
Height of the mass m_1	z_1	Optimized
Height of the hip	z_2	$0.95(L_{shin} + L_{thigh})$
Step time	T	0.7 s
Step length	D_s	0.4 m
Calculus variable	ω	$\pi/(5T)$
Calculus variable	$\lambda = \gamma$	z_2/z_1

Using the developed simulator, four simulation scenarios are proposed to validate the proposed optimal pattern generator, namely:

- *Simulation 1*: optimal trajectories generation for straight walking,
- *Simulation 2*: trajectories generation for walking with change of direction without optimisation,
- *Simulation 3*: trajectories generation for walking with a change of direction and optimization.
- *Simulation 4*: Effects of walking parameters

These simulations will be detailed and commented in the following.

6.1 Simulation 1: straight walking

The optimization criterion given in (24) is used to find the best values for z_1 and m_1 using the `fminsearch` algorithm proposed within Matlab software. The optimization algorithm uses a simplex search method described in [23]. The obtained optimization results are coherent with their physical meanings: the masses are found to be positive and the positions of the three masses are inside the convex envelope of the robot. The obtained optimal solution is summarized in Tab. 3, and the simulation results are illustrated, for six walking steps, through curves of Figs. 12–18.

Tab. 3. Resulting optimized parameters.

Parameter	Without optimization	With optimization
z_1	0.6 m	0.2598 m
m_1	6 kg	0.4442 kg

Figures 12 and 13 represent respectively the evolution of the joints' positions and velocities, where it can clearly be seen that the obtained trajectories are periodic. Furthermore the trajectories of one leg are symmetrical w.r.t. those of the other one.

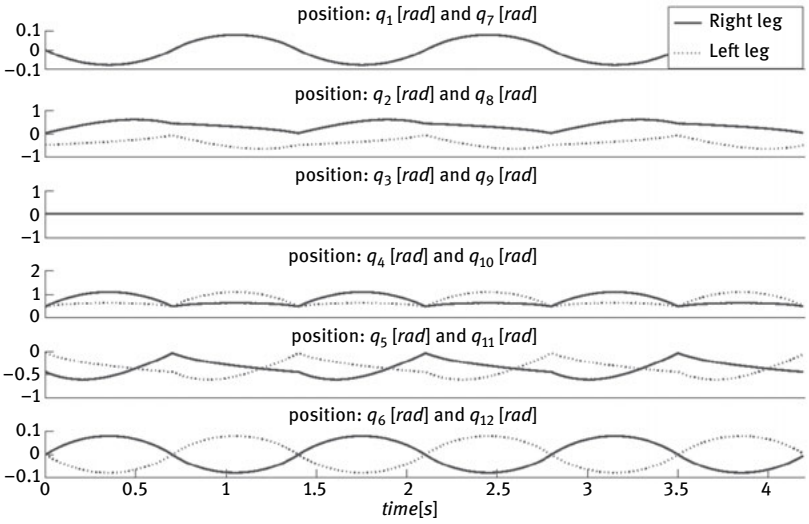

Fig. 12. Joints' positions generated by the proposed optimal pattern generator.

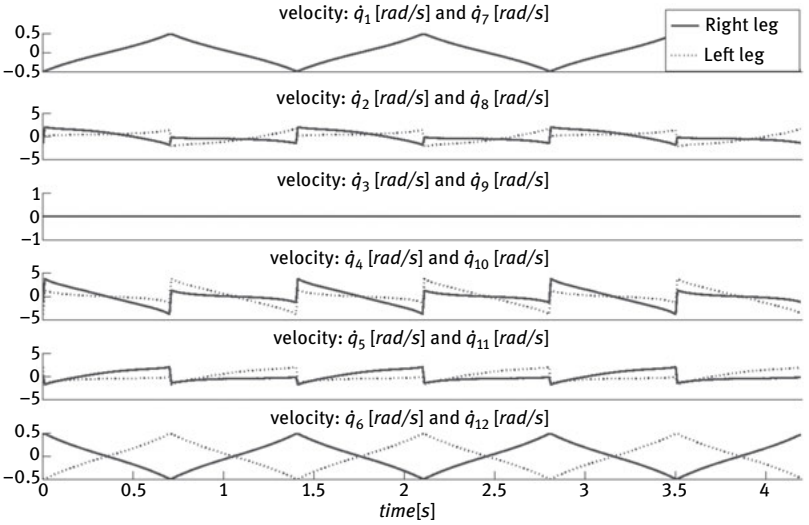

Fig. 13. Joints' velocities generated by the proposed optimal pattern generator.

Figures 14, 15 and 16 represent the evolution of the ZMP and the CoM positions with respect to the footprints of the biped robot on the ground generated respectively by the linear inverted pendulum model (LIPM), the original (3MLIPM) pattern generator proposed in [17] and the optimal one proposed in this paper.

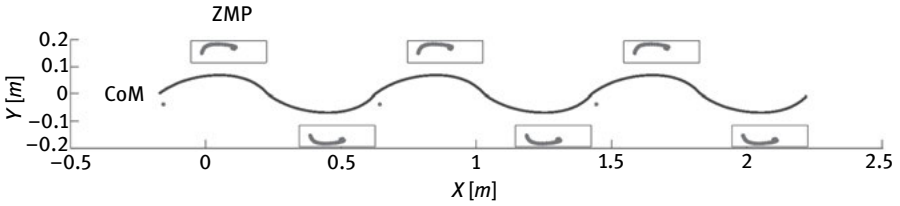

Fig. 14. Evolution of ZMP and CoM trajectories with the LIPM.

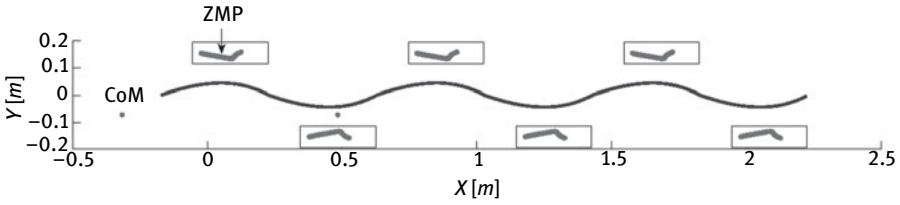

Fig. 15. Evolution of ZMP and CoM trajectories with the original 3MLIPM.

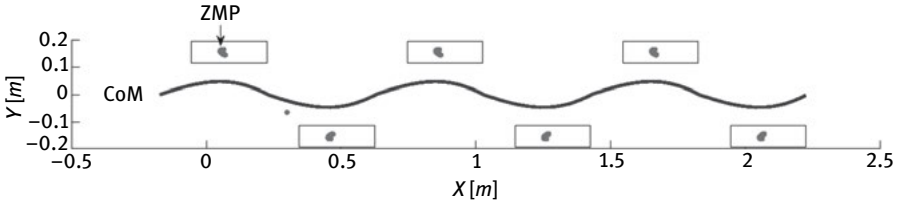

Fig. 16. Evolution of ZMP and CoM trajectories with the proposed optimal 3MLIPM.

The ZMP position calculation is issued from an angular momentum evaluation based on Kajita's formulation [20]. This computation is not base on the simplified three-mass model; indeed, it uses the dynamic model of the biped robot to produce a realistic ZMP evaluation.

For the LIPM as well as the original 3MLIPM, the ZMP moves inside the footprint with a big variation, however when the optimal parameters are used, the ZMP is more concentrated in the center of the footprint and the stability margins are better.

Therefore, the walking dynamic stability is clearly improved with the proposed optimal 3MLIPM pattern generator due to the increase of the stability margins.

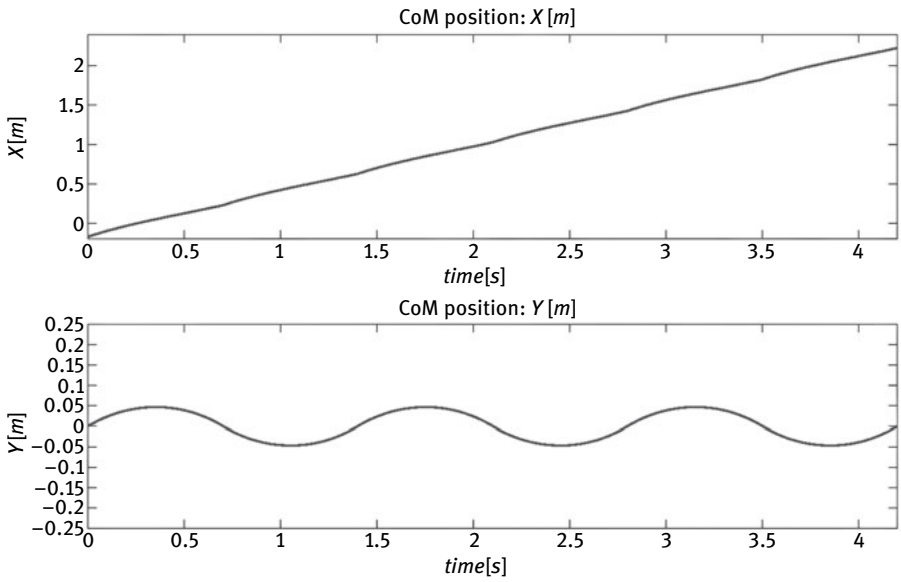

Fig. 17. CoM evolution versus time with optimization.

Figure 17 displays the evolution of the position of the CoM along the x and y axes during walking. The obtained trajectories are cyclic along the y axis with a reduced amplitude thanks to the optimal parameters. Figure 18 shows the trajectories of movement of the swing foot for one step.

6.2 Simulation 2: walking with a change of direction

The objective of this simulation is to evaluate the stability margins of the pattern generator proposed in [17] in case of a change of direction during walking. The obtained result is depicted in Fig. 19 where it is worth to note that the change of direction during walking has not been yet considered in the original 3MLIPM, therefore a simple simulation shows a loss of stability during walking while turning.

Indeed, when the robot changes the walking direction, the position of the ZMP is moving within footprints, being sometimes outside of the stance footprint, therefore the robot becomes unstable. Consequently, a computation of optimal parameters in this scenario will be necessary to improve the dynamic walking stability. This is the objective of the next simulation scenario.

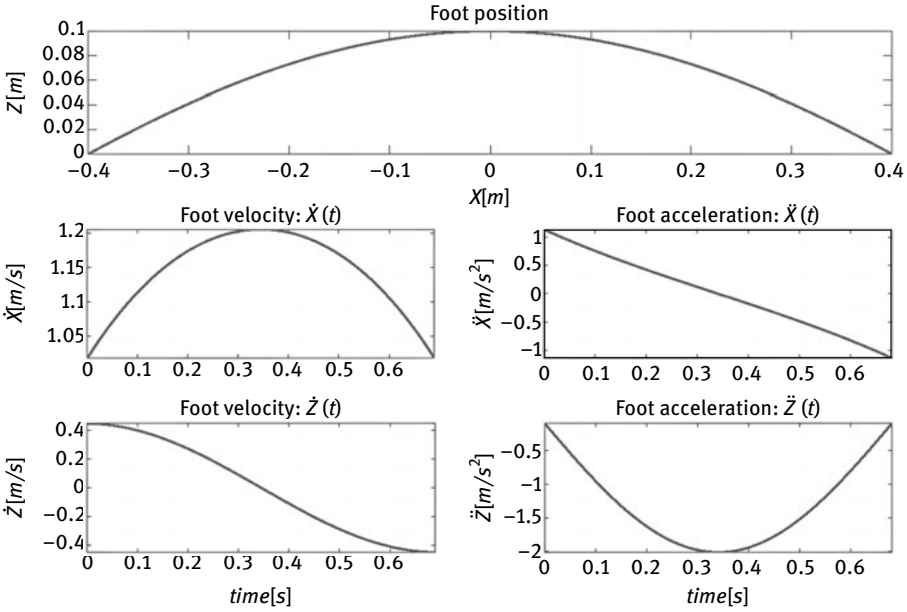

Fig. 18. Evolution of the swing foot trajectories.

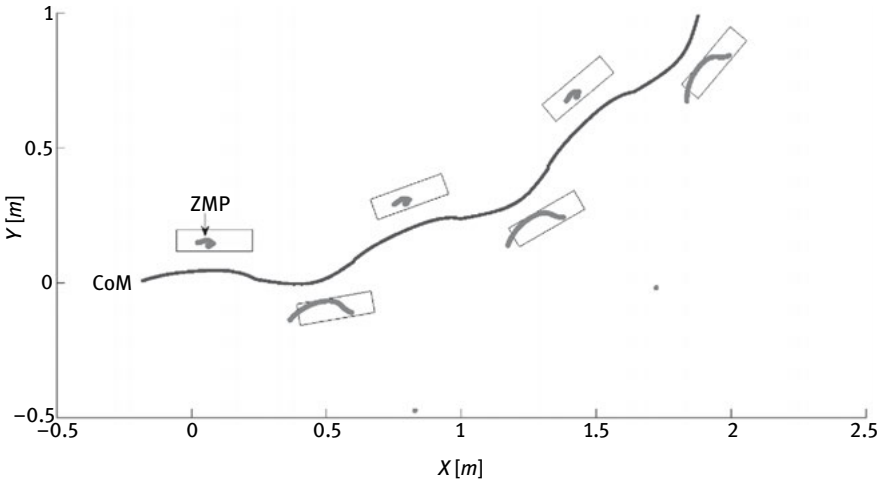

Fig. 19. Evolution of ZMP and CoM trajectories with change of direction.

6.3 Simulation 3: change of direction with optimization

In the proposed optimal pattern generator, the optimization process computes the best values of the parameters z_1 and m_1 and uses them to generate the joints' trajectories.

Figures 20 and 21 represent respectively the evolution of the new joints' positions and velocities for this scenario. Theses trajectories allow a rotation of the biped robot during walking.

Figure 22 represents the evolution of the ZMP and the CoM positions as well as the footprints of the biped robot on the ground level when turning with an angle of 20 degrees at each walking step.

With the proposed optimization, as illustrated in Fig. 22, the robot remains stable during walking while turning since it keeps the ZMP always inside the footprint of the supporting leg.

According to the obtained results, from simulation 1 and 3, it is clearly shown that the proposed optimal pattern generator has significantly improved the dynamic stability of the biped robot for both scenarios: straight walking and change of direction.

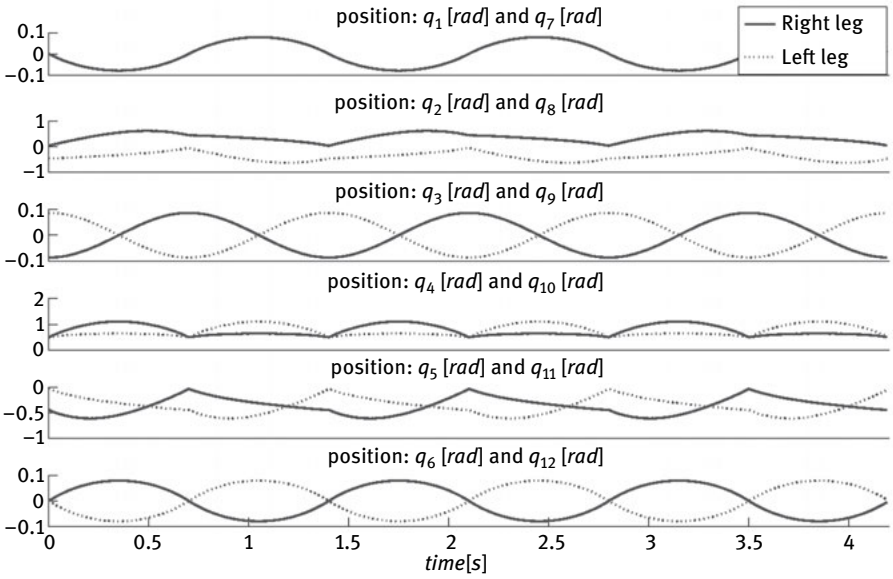

Fig. 20. Joints' positions with change of direction generated by the proposed optimal pattern generator.

6.4 Simulation 4: effects of walking parameters

The optimal values summarized in Tab. 3 are used to compute stability margins Mx and My for straight walking with different step lengths and the objective is to analyze the sensitivity of the model w.r.t. step length variation.

The optimal values of mass distribution have been calculated with a step length of $0.4\ m$. These values are then used with different step lengths Ds. The corresponding stability margins are summarized in Tab. 4. It is worth to note that the modification of the step length don't induce a loose of stability during walking. The optimal mass distribution make the proposed pattern generator less sensitive to step length variations.

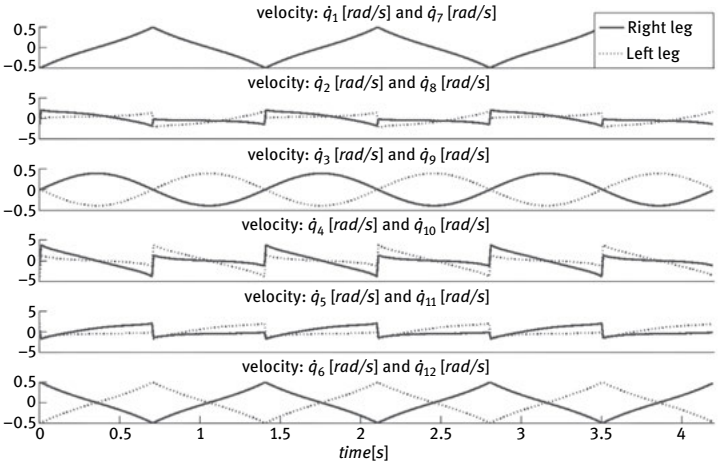

Fig. 21. Joints' velocities with change of direction generated by the proposed optimal pattern generator.

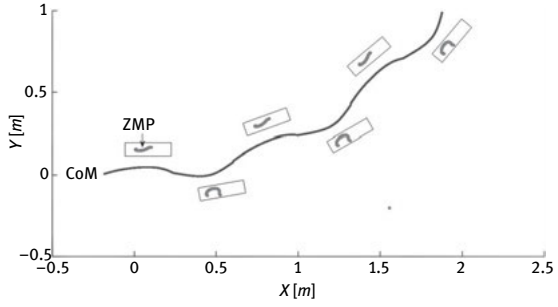

Fig. 22. Evolution of ZMP and CoM trajectories in case of change of direction generated by the proposed optimal pattern generator.

Tab. 4. Step length influence on stability margins

Ds	0.1	0.2	0.3	0.4	0.5
Stability	stable	stable	stable	stable	stable
Mx	0.105	0.108	0.110	0.112	0.115
My	0.028	0.029	0.030	0.030	0.029

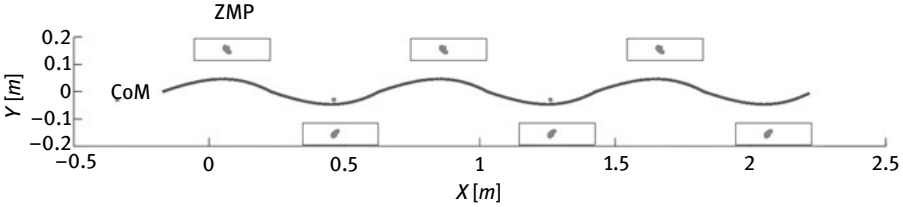

Fig. 23. Evolution of ZMP and CoM trajectories with $Ds = 0.4$.

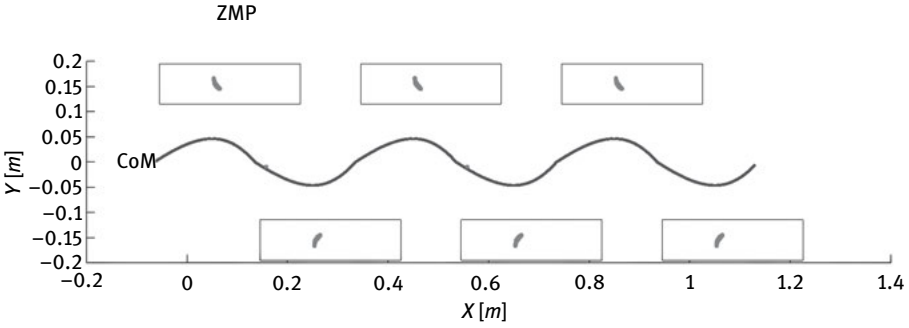

Fig. 24. Evolution of ZMP and CoM trajectories with $Ds = 0.2$.

7 Conclusions and future work

The objective of this work was to generate stable dynamic walking for SHERPA biped robot. To deal with this problem, the original pattern generator proposed in [17] based on a Three-Mass Linear Inverted Pendulum Model has been extended with a ZMP-based optimization to improve dynamic walking stability. The optimization use a ZMP based performance index in an optimization problem whose solution gives the best values of the model's parameters w.r.t. dynamic walking stability computed using a whole body model. The case of change of direction during walking has also been studied and stability in this case has been enhanced thanks to the optimization.

Several numerical simulations have been presented to show the effectiveness of the proposed optimal pattern generator for the case of the biped walking robot SHERPA.

Future works can include real-time implementation of the proposed method on the prototype of SHERPA biped robot and the creation of a motion database to be able to change the walking speed of the robot in real-time.

Acknowledgments: This research was supported by the French National Research Agency, within the project R2A2 (ANR-09-SEGI-011).

Bibliography

[1] S. Ma, T. Tomiyama, and H. Wada. Omnidirectional static walking of a quadruped robot. *IEEE Trans. on Robotics*, 21(2):152–161, 2005.

[2] M. Vukobratovic and B. Borovac. Zero-moment point-thirty five years of its life. *Int. J. of Humanoid Robotics*, 1(1):157–173, 2004.

[3] P. Sardain and G. Bessonnet. Forces acting on a biped robot. Center of pressure-zero moment point. *IEEE Trans. on Systems, Man and Cybernetics, Part A: Systems and Humans*, 34(5):630–637, 2004.

[4] A. Goswami. Postural stability of biped robots and the foot-rotation indicator (FRI) point. *Int. J. of Robotics Research*, 18(6):523–533, 1999.

[5] K. Harada, K. Miura, M. Morisawa, K. Kaneko, S. Nakaoka, F. Kanehiro, T. Tsuji, and S. Kajita. Toward human-like walking pattern generator. *IEEE/RSJ Int. Conf. on Intelligent robots and systems (IROS'09)*, (Albuquerque, NM, USA), :1071–1077, 2009.

[6] Q. Huang, S. Kajita, N. Koyachi, K. Kaneko, K. Yokoi, H. Arai, K. Komoriya, and K. Tanie. A high stability, smooth walking pattern for a biped robot. *IEEE Int. Conf. on Robotics and Automation (ICRA'99)*, :65–71, Detroit, Michigan, USA, 1999.

[7] J. Yamaguchi, E. Soga, S. Inoue, and A. Takanishi. Development of a bipedal humanoid robot-control method of whole body cooperative dynamic biped walking. *IEEE Int. Conf. on Robotics and Automation (ICRA'99)*, 1:368–374, Detroit, Michigan, USA, 1999.

[8] S. Kajita, F. Kanehiro, K. Kaneko, K. Fujiwara, K. Yokoi, and H. Hirukawa. Biped walking pattern generation by a simple three-dimensional inverted pendulum model. *Advanced Robotics*, 17(2):131–147, 2003.

[9] Z. Tang and M. Er. Humanoid 3D Gait Generation Based on Inverted Pendulum Model. *IEEE 22nd Int. Symp. on Intelligent Control (ISIC'07)*, :339–344, Singapore, 2007.

[10] S. Kajita, F. Kanehiro, K. Kaneko, K. Yokoi, and H. Hirukawa. The 3D Linear Inverted Pendulum Mode: A simple modeling for a biped walking pattern generation. *IEEE/RSJ Int. Conf. on Intelligent Robots and Systems (IROS'01)*, :239–246, Maui, Hawaii, USA, 2001.

[11] S. Feng and Z. Sun. A simple trajectory generation method for biped walking. 10th *Int. Conf. on Control, Automation, Robotics and Vision (ICARCV'08)*, :2078–2082, 2 Hanoi, Vietnam, 008.

[12] S. Kajita, F. Kanehiro, K. Kaneko, K. Fujiwara, K. Harada, K. Yokoi, and H. Hirukawa. Biped walking pattern generation by using preview control of zero-moment point. *IEEE Int. Conf. on Robotics and Automation (ICRA'03)*, 2:1620–1626, 2003.

[13] A. Albert and W. Gerth. Analytic Path Planning Algorithms for Bipedal Robots without a Trunk. *J. of Intelligent and Robotic Systems*, 36(2):109–127, 2003.

[14] J. Park and K. Kim. Biped robot walking using gravity-compensated inverted pendulum mode and computed torque control. *IEEE Int. Conf. on Robotics and Automation (ICRA'98)*, :3528–3533, Leuven, Belgium, 1998.
[15] J. Kanniah, Z. Lwin, D. Kumar, and N. Fatt. A ZMP management scheme for trajectory control of biped robots using a three mass model. *Proceedings of the 2nd Int. Conf. on Autonomous Robots and Agents (ICARA'04)*, :458–463, Palmerston North, New Zealand, 2004.
[16] T. Buschmann, S. Lohmeier, M. Bachmayer, H. Ulbrich, and F. Pfeiffer. A collocation method for real-time walking pattern generation. *IEEE/RAS Int. Conf. on Humanoid Robots*, :1–6, 2007.
[17] S. Feng and Z. Sun. Biped robot walking using three-mass linear inverted pendulum model. *Proceedings of the Int. Conf. on Intelligent Robotics and Applications (ICIRA'08)*, :371–380, Springer-Verlag, Wuhan, China, 2008.
[18] `http://www.lirmm.fr` [Online].
[19] I. M. C. Olaru, S. Krut, and F. Pierrot. Novel mechanical design of biped robot sherpa using 2 dof cable differential modular joints. *Proceedings of the 2009 IEEE/RSJ Int. Conf. on Intelligent Robots and Systems (IROS'09)*, :4463–4468, St. Louis, MO, USA, 2009.
[20] S. Kajita, H. Hirukawa, K. Harada, and K. Yokoi. *Introduction à la commande des robots humanoides. Translated in French by Sakka, S*. Springer, 2009.
[21] S. Kajita, F. Kanehiro, K. Kaneko, K. Fujiwara, K. Yokoi, and H. Hirukawa. A realtime pattern generator for biped walking. *IEEE Int. Conf. on Robotics and Automation, ICRA'02*, 1:31–37, IEEE, 2002.
[22] J. T. Kim and J. H. Park. Quick change of walking direction of biped robot with foot slip in single-support phase. 11th *IEEE-RAS Int. Conf. on Humanoid Robots (Humanoids'11)*, :339–344, 2011.
[23] J. C. Lagarias, J. A. Reeds, M. H. Wright, and P. E. Wright. Convergence properties of the Nelder–Mead simplex method in low dimensions. *SIAM J. on Optimization*, 9(1):112–147, 1998.

Biographies

David Galdeano
received the M.S. degree in Robotics and Automation from the University Montpelier 2, France, in 2010. Currently he is a Ph.D. student in the Laboratory of Informatics, Robotics, and Microelectronics (LIRMM). His current research interests include humanoid robotics, whole-body posture control.

Ahmed Chemori
received his MSc and PhD degrees respectively in 2001 and 2005, both in automatic control from the Grenoble Institute of Technology. He has been a Post-doctoral fellow with the Automatic control laboratory of Grenoble in 2006. He is currently a tenured research scientist in Automation and Robotics at the Montpelier Laboratory of Informatics, Robotics, and Micro-electronics. His research interests include nonlinear, adaptive and predictive control and their applications in humanoid robotics, underactuated systems, parallel robots, and underwater vehicles.

Sébastien Krut
received the M.S. degree in mechanical engineering from the Pierre and Marie Curie University, Paris, France, in 2000 and the Ph.D. degree in automatic control from the Montpelier University of Sciences, Montpelier, France, in 2003. He has been a Post-doctoral fellow with the Joint Japanese-French Robotics Laboratory (JRL) in Tsukuba, Japan in 2004. He is currently a tenured research scientist in Robotics for the French National Centre for Scientific Research (CNRS), at the Montpelier Laboratory of Computer Science, Microelectronics and Robotics (LIRMM), Montpelier, France. His research interests include design and control of robotic systems.

Philippe Fraisse
received M.Sc degree in Electrical Engineering from Ecole Normale Superieure de Cachan in 1988. He received Ph.D. degree in Automatic Control in 1994. He is currently Professor at the University of Montpelier, France. He is the head of robotics department (LIRMM) and co-chair of French National Workgroup (GDR Robotique) working on Humanoid Robotics (GT7). He is also member of JRL-France scientific board (Japanese- French joint Laboratory for Robotics, AIST-JRL) and member of IEEE. His research interests include modeling and control applied to robotic and rehabilitation fields, including humanoid robotics, robotics for rehabilitation.